Isı Bilimi ve Tekniği Dergisi, 36, 1, 69-82, 2016
J. of Thermal Science and Technology

ISSN 1300-3615

3-D NUMERICAL INVESTIGATION AND OPTIMIZATION OF CENTRIFUGAL SLURRY PUMP USING COMPUTATIONAL FLUID DYNAMICS

Mehmet Salih CELLEK* and Tahsin ENGIN **
*Heat and Thermodynamics Division, Department of Mechanical Engineering, Mechanical Engineering Faculty, Yildiz Technical University, 34349 Besiktas, Istanbul, mscellek@yildiz.edu.tr
**Department of Mechanical Engineering, Applied Fluid Mechanics Laboratory, Faculty of Engineering, Sakarya University, 54187 Sakarya, tengin@sakarya.edu.tr

(Geliş Tarihi: 03.02.2015, Kabul Tarihi: 23.11.2015)

Abstract: Energy conversion applications are directly affected through the employment of turbomachines and their efficiencies. Energy importance and wide-spread application of turbomachines, make it crucial to optimize their components. In order to optimizastion, the actual flow field and the interaction between the components must be revealed as 3-D studies. Although many studies have focused on the component optimization, mainly volute and impeller in water pumps, there is no systematic elaboration of the same methodology for centrifugal slurry pumps.
The purpose of this paper is to improve the performance of a centrifugal slurry pump by means of Computational Fluid Dynamics (CFD). Therefore, an extensive parametric study has been carried out in order to optimize the shroud type impeller taking into account the blade discharge angle (β_2), addition splitter blades and modified blade (backward long blades). Additionally, the tongue region of the original pump is re-designed. The results obtained in this study show that it is possible to improve the performance of the impeller and the volute of the centrifugal slurry pump by choosing correct parameters. From the analysis point of view, it is demonstrated numerically that the hydraulic efficiency of the centrifugal slurry pump can be increased up to 9% by using the backward long blades in addition to modified volute compared to the original ones. The last stage of the study focuses on the performance of slurry pump while handling slurry mixture at different concentrations in comparison with clear water as a case study. The flow pattern is visualized with the instantaneous pressure contours and the velocity streamlines. Furthermore, the characteristic performance curves of each pump are compared and discussed. The numerical solutions of the discredited three-dimensional, incompressible Navier-Stokes equations over the structured mesh are accomplished with commercial software Fluent®.
Keywords: Slurry pump, Blade angle, Splitter blade, Parametric study, Optimization.

HESAPLAMALI AKIŞKANLAR DİNAMİĞİ (HAD) KULLANILARAK ÜÇ BOYUTLU SANTRİFÜJ ÇAMUR POMPASININ SAYISAL OLARAK İNCELENMESİ VE OPTİMİZASYONU

Özet: Enerji dönüşüm uygulamaları, kullanılan türbomakinaların ve verimlerinden direk olarak etkilenmektedir. Enerjinin önemi ve türbomakinaların geniş uygulama alanı, türbomakinaların bileşenlerinin optimizasyonunu çok önemli kılar. Optimizasyon için, gerçek akış alanı ve türbomakina bileşenleri arasındaki etkileşim 3 boyutlu çalışmalar olarak ortaya konması gerekir. Birçok çalışma su pompalarının bileşenleri olan salyangoz ve çark optimizasyonuna odaklanmasına rağmen, santrifüj çamur pompaları için aynı sistematik metodoloji ve çalışma mevcut değildir. Bu çalışmanın amacı Hesaplamalı Akışkanlar Dinamiği (HAD) vasıtasıyla santrifüj çamur pompasının performansını iyileştirmektir. Bu nedenle, kapalı tip çarkın optimizasyonu için kanat çıkış açısı, ara kanatçık eklenmesi ve kanadın modifiye edilmesi göz önünde bulundurularak kapsamlı bir parametrik çalışma yürütülmüştür. İlave olarak, orijinal pompanın salyangoz dil bölgesi tekrar tasarlandı. Bu çalışmadan elde edilen sonuçlar göstermiştir ki doğru parametrelerin seçilmesiyle santrifüj çamur pompası çarkı ve salyangozunun performanslarının artırılması mümkündür. Sayısal olarak elde edilen analiz sonuçlarına göre, çamur pompasının hidrolik verimi geriye eğimli uzun kanatlı çark ve ilk duruma göre modifiye edilmiş salyangozun kullanılmasıyla % 9'a kadar artırılabilir. Çalışmanın son bölümü bir durum çalışması olarak temiz su ile karşılaştırıldığında farklı konsantrasyonlarda çamur karışımı iletilirrken çamur pompasının performansı üzerinde duruluyor. Akış şekli anlık basınç konturları ve hız akım çizgileri ile görselleştirilmiştir. Dahası her bir pompanın karekteristik performans eğrileri karşılaştırıldı ve tartışıldı. Ayrıklaştırılmış, üç boyutlu, sıkıştırılamaz Navier-Stokes denklemlerinin sayısal çözümleri yapılandırılmış ağ kullanılarak ticari yazılım Fluent ile gerçekleştirilmiştir.
Anahtar Kelimeler: Çamur pompası, kanat açısı, Ara kanatçık, Parametrik çalışma, Optimizasyon

NOMENCLATURE

b	blade height [m]
C	concentration of solids
d_1	impeller suction diameter [m]
d_2	impeller outlet diameter [m]
d_{wn}	particle size (diameter) [μm]
g	gravity [m/s^2]
t	blade thickness [m]
β_1	impeller blade outlet angle [°]
β_2	blade outlet angle [°]
k	turbulance kinetic energy [m^2/s^2]
K	reduction factor
ε	turbulance dissipation rate [m^2/s^3]
z	blade number
p	pressure [N/m^2]
S	solid specific gravity
u	velocity [m/s]
ρ	density [kg/m^3]
ω	rotating speed [rad/s]
μ	viscousity [kg/m· s]
σ	Prandtl number
P_{sh}	shaft power [W]
T	torque [N.m]
n	number of revolutions per minute [s^{-1}]
Q	flow rate [m^3/h]
t	relative error
η	pump efficiency

Subscripts

eff	dynamic effective viscosity
H	head reduction factor
t	turbulance viscosity
k	prandtl number for k
v	volumetric concentration
w	weight concentration
ε	prandtl number for ε
η	efficiency reduction factor

INTRODUCTION

A slurry mixture can include very fine particles which can form stable homogeneous mixtures named non-settling slurries or coarser particles which tend to have higher wearing properties and disposed to form an unstable mixture named settling slurries. The combination of the size, shape, type and quantity of the particles determine the exact characteristics and flow properties of the slurry flow. Therefore a special attention must be given to flow and pump selection (Warman International Ltd., 2000).

Due to many advantage and superiority among others such as consider impeller size and design, their ease of maintenance, the type of shaft seal to be used and the choice of the optimum materials, centrifugal slurry pumps have been employed widely for slurry transportation for years (Warman International Ltd., 2000; Gandi et al., 2001; Singh et al., 2011; Engin, 2000). But they are needed to withstand wear caused by the abrasive, erosive and often corrosive attack on the materials. Slurry pumps therefore need heavier impellers to accommodate the passage of large particles. They must also be constructed in special blade number and design and materials to withstand the internal wear caused by the solids (Warman International Ltd., 2000).

Turbomachines such as pumps, fans, turbines and compressors are extensively used in the industry and buildings for generating or consuming of energy. Specific turbomachines are utilized for energy production purposes such as steam and water turbines, while other types including fans, compressors and pumps consume energy to increase the fluid pressure. Due to their common use and the importance of the energy, the optimization will be a pivotal requirement.

Recent developments in the Computational Fluid Dynamics (CFD) lead to specific important facilities to design turbomachines with the complex and the high turbulence internal flows. Thus, it allows interpreting the design procedure and optimizing the product components without the high cost and less waste of time before the manufacturing process. Besides, it enables us to study the effects of various parameters on these components. The accuracy of the CFD method has been proven by many researchers for years (Sun and Tsukamoto, 2001; Gonzalez et al., 2002; Bacharoudis et al., 2008). This approach is widely used in turbomachines. Rajendran and Purushothaman (2012) discussed circumstantially the flow pattern, the pressure distribution in the blade passage, the blade loading and the pressure plots in a centrifugal pump impeller using three dimensional Navier-Stokes code called CFX. Kyparissis et al. (2009) numerically examined simple and double-arc blade design methods taking into account the one dimensional Pfleiderer's analytical approach. Subsequently, optimizing of the hydrodynamic efficiency of a centrifugal pump with the different blade models became possible by employing CFD. Based on the study of Li (2011), a singularity method was applied for inversely designing impeller blades. The hydraulic efficiency of the original impeller was increased by 5% at the design duty and 9% at the off design condition with the inverse design method. Zhou et al. (2003) investigated the performance of centrifugal pumps with three different impeller (one has four straight blade and the other two have six twisted blades) with the commercial CFX with the use of the standard $k-\varepsilon$ turbulence model. It was concluded from the study that the predicted results relating to the twisted-blade impeller were better than those relating to the straight blade impeller. Cui et al. (2006) studied the effects of the splitter blades on the performance of the long blade impeller while operating at high speed. In their numerical analysis, the commercial code FINE/TURBOTM 6.2 was used to calculate Navier-Stokes equations with the one equation Spalart-Allmaras turbulence model. They concluded that the backflow region, whose center was near the suction-side, experienced a minor change through adding mid

and short splitter blades. They also stated that with the large number of the splitter blades, the increase of pressure would be the largest capacity in the whole range. In addition, splitter blades neither can effectively solve the small flow instability nor the backflow in the impeller. Madhwesh et al. (2011) investigated the impact of the splitter blade at different locations on the impeller of a centrifugal fan. The results exhibited that the splitter blade provided at the impeller leading edge provides pressure recovery of the fan outlet. However, there is not a significant static pressure recovery at the trailing edge near the suction side and the circumferential mid-span of the splitter blades. When the splitter blades located at the trailing edge near the pressure side of the main blades, the static pressure almost decreases. Sheng et al. (2012) studied the effects of splitter blades on a centrifugal pump which can be operated reversely similar to turbines known as PAT. From the analysis, they concluded that the splitter blades being added to the impeller flow passage increased the efficiency of the PAT. Besides, the splitter blades had significant effects in decreasing of the pressure fluctuations. Another splitter blades application was carried out by Kergourlay et al. (2007). In their study, two impellers with and without splitter blades were designed to reveal the influence of the splitter blades on the pump performance numerically and experimentally. They declared that the splitter blades had positive and negative impacts on the pump performance. Firstly, they increase the pump head compared to the original impeller. Secondly, the most important effect is that they also diminish the pressure fluctuations which cause the distributed noise and vibration accelerations. On the other hand, the addition of the splitter blades does not improve the efficiency because of the greater hydrodynamics losses. From the Rababa (2011) studied the effects of number of blades and created the splitter blades with the various blade widths by $1/1$, $2/3$ and $1/3$ on the open type impeller performance of groundwater centrifugal pumps. In this study, the performance of the four blade impeller was better than two and three blade impellers. On the other hand, from the experimental results of his study, the splitter blades by $1/1$ blade width increased the pump head by 4% and the efficiency by %1. However the splitter blades by $2/3$ and $1/3$ blade width had no effect on the characteristic curve of the $H-Q$. Unlike the water pumps, a slurry pump is used for transportation of slurries through long distance pipeline systems. Because of the effects of slurries in the mixture, the performance of a centrifugal slurry pump differs from a pump operating with clean water (Kazim et al., 1997; Cader et al., 1994). Das et al. (2011) studied two dimensional flow phenomenon of a centrifugal slurry pump while it handles the clean water from shut-off to the maximum flow rate comparing with the experimental data. They emphasize that blade parameters such as the number and thickness of the blades can be investigated because of their importance for the centrifugal slurry pump. Singh et al. (2011) had evaluated the performance characteristics of the centrifugal slurry pump with bottom ash with different concentrations. They observed numerically that the head and the efficiency of centrifugal slurry pump decrease with increase in solid concentration. Baocheng and Wei (2014) studied a 3D turbulence flow in a low specific speed solid-liquid centrifugal pump with volume fraction of %10, %20 and %30 for the same particle diameter (0.1 mm). Also, they underlined that iteration convergence problem occurred by the high rotational speed and highly complex internal structure. They cope with this problem by changing underrelaxation factors. Although there are many valuable papers available to optimize the centrifugal water pumps and their impellers state above; the optimization of centrifugal slurry pump impellers is rather limited in the literature.

In this work, an extensive parametric study has been carried out in order to optimize the shroud type impeller of an original centrifugal slurry pump. With the use of ANSYS-CAD parametric interface feature, three impellers have been created to investigate the effects of blade exit angle (β_2) . Furthermore, the effects of splitter blades by 1/2 and 1 times the blade height on the parametric impeller (β_2= 25° impeller) are investigated. Additionally, the leading edge and curvature of the β_2= 25° impeller blade is modified. On the other hand, the tongue region of the slurry pump is modified to prevent the back flow in the gap between the impeller and the volute. For each impeller, the fluid flow field visualized with the instantaneous pressure contours and the streamlines inside the pump. Also the pump performance curves for each pump are compared and discussed. The computational fluid dynamics analysis is performed with the commercial software Fluent (2005).

THEORETICAL MODEL

Pump Geometry and Impellers

A centrifugal slurry pump with a shrouded type impeller of which geometrical dimensions provided by Tufekcioglu Kaucuk Ltd (2013) is considered to study as shown in Fig.1. The original impeller of this pump is re-designed for parametric study used the simple-arc blade design method (SAM) according to the Pfleiderer (1961) blade theory as shown in Fig. 2. Therefore the blade exit angle applied to blade center line can be changed without re-designing.

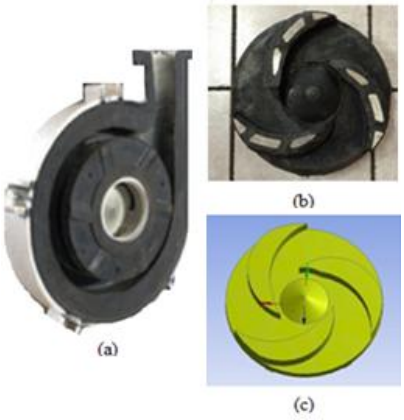

Figure 1. Original rubber coated centrifugal slurry pump (a) and impeller (b), impeller's CAD model (c) without shrouds

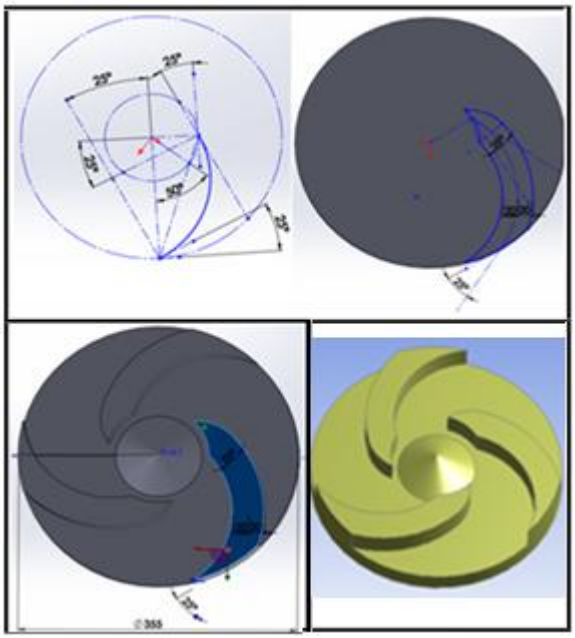

Figure 2.The parametric impeller (β_2= 25°), created step by step by means of Pfleiderer (1961) blade theory

To optimize the slurry pump performance, initially three different impellers were created to investigate the effects of outlet blade angle β_2= 20°, 25°, and 40°, then the β_2= 25° impeller were modified with the addition of splitter blades by 1/2 and 1 times the blade height. The splitter blades whose exit angle (β_2) and thickness were 32° and 15 mm, respectively located approximately in the middle of the flow passage. Lastly, one impeller was created with backward long blades taken into account the fluid flow field inside the impeller during the post process of the β_2= 25° impeller. Created impellers are shown in Fig.3.

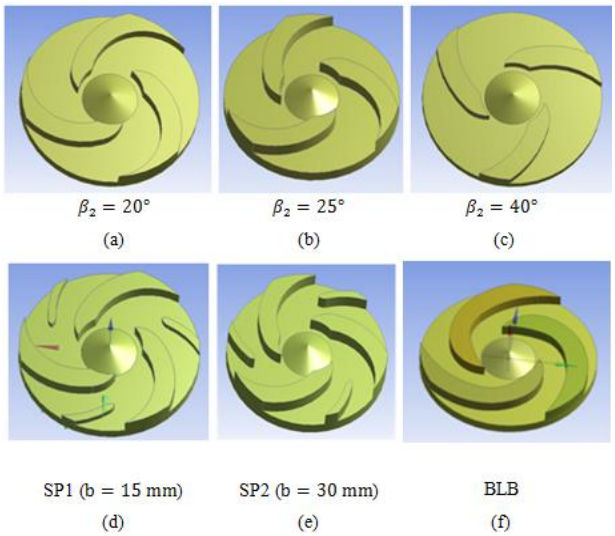

Figure 3. Parametric impeller is modified with different outlet angles (β_2) (a), (b), (c), splitter blades (d), (e) and backward long blades (f), the shrouds are hided

The geometrical dimensions of the centrifugal slurry pump impellers investigated in this study are listed in Table 1.

Table 1: Dimensions of original and parametric impellers (β_2= 25°).

Impeller Parameters	Unit	Original impeller	Parametric impeller
Blade number, (z)	-	3	3
Blade height, (b)	mm	30	30
Suction diameter,(d1)	mm	130	130
Outlet diameter, (d2)	mm	355	355
Outlet angle,(β_2)	℃	30	25
Blade thickness, t	mm	50	40

2.2. Mesh Generation

In the present study, both structured and unstructured meshes were studied for mesh independence presented in Table 2. To investigate the effects of blade exit angle, splitter blades and backward long blades, fine structured mesh type used with 2030645 total mesh number. Inflation layer meshing was applied to the boundary layer region with ten layers to capture the flow separation, pressure drop, and adverse pressure gradients inside the impeller with sufficient number of mesh elements shown in Fig. 4.

Table 2: Mesh independence of the = 25° impeller

Mesh type	Turbulence model	Total mesh number	Head, H (m)	Efficiency,η
Structured mesh	k-ε	3525644	15.96	0.645
Structured mesh	k-ε	2209864	15.94	0.644
Structured mesh	SST	2209864	16.10	0.646
Structured mesh	k-ε	2030645	15.97	0.646
Unstructured mesh	k-ε	1076125	15.83	0.655

The whole pump geometry consists of three main zones; inlet, impeller and volute zones. The inlet zone is the simplest one which the flow is entering and consists of 32961 mesh elements. The case zone, which consists of 865578 mesh elements is just as critical as the impeller for converting velocity to pressure. The most important zone of the pump is rotating impeller, which converts the mechanical energy to kinetic energy. This zone consists of 1132106 mesh elements for the β_2= 25° impeller. Although mesh elements number used for the β_2= 25° impeller is 1132106, it differs for other impellers.

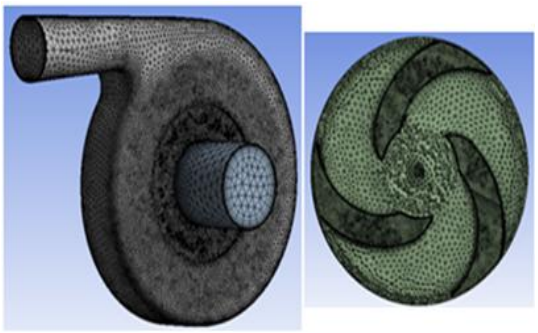

Figure 4. Structured mesh generations of the fluid domain with ten inflation layers around blades, (the shroud is hided)

Governing Equations and Boundary Conditions

In this study, the Reynolds-averaged Navier-Stokes equation was calculated by means of commercial software package Fluent that helps in achieving a finite volume approach for the solutions (Singh and Nataraj, 2012). The steady and three dimensional incompressible flow through the rotating impeller solved in a moving reference with constant rotational speed. Moreover the flow through the stationary parts of the pump is solved in an inertial reference frame. The governing equations for the rotating impeller and stationary parts of the pumps are formulated as follows, neglecting the energy equation and the gravity (Bacharoudis et al., 2008).

$$\nabla\rho\,\mathbf{u_r} = 0 \quad (1)$$

$$\nabla\rho\mathbf{u_r} = 2\rho\boldsymbol{\omega}\times\mathbf{u_r} + \rho\boldsymbol{\omega}\times\boldsymbol{\omega}\times r = -\nabla p + \mu_{eff}\nabla^2 \quad (2)$$

$$\nabla\rho\mathbf{u} = -\nabla p + \mu_{eff}\nabla^2\mathbf{u} \quad (3)$$

where $\mathbf{u_r}$ is the velocity vector in a rotating system, on the other hand $\mathbf{u}$ is the local vector in the stationary frame of reference, $\boldsymbol{\omega}$ is the rotational speed, p is the pressure, μ_{eff} is the dynamic effective viscosity which is a linear combination of laminar and turbulent viscosity derived from $k-\varepsilon$ model of turbulence. Standard $k-\varepsilon$ turbulence model, which has been widely utilized for the prediction of turbulence, is selected because of the capability and satisfactory results in the turbomachinary (Singh and Nataraj, 2012; Li, 2012; Safikhani et al., 2011; Engin, 2006; Versteeg and Malalasekera, 1998).

The turbulence kinetic energy (k) and turbulence dissipation rate (ε) can be presented with the differential transport equations as follows (Bacharoudis et al., 2008).

$$\nabla\rho\mathbf{u}k = \nabla\left(\left(\mu+\frac{\mu_t}{\sigma_k}\right)\nabla k\right) + G_k - \rho\varepsilon \quad (4)$$

$$\nabla\rho\mathbf{u} = \nabla\left(\left(\mu+\frac{\mu_t}{\sigma}\right)\nabla\right) + C_{1\varepsilon}\frac{\varepsilon}{k}G_k - C_{2\varepsilon}\rho\frac{\varepsilon^2}{k} \quad (5)$$

$$\mu_t = \rho C_\mu \frac{k^2}{\varepsilon} \quad (6)$$

where $\mathbf{u}$ stands for velocity component in the corresponding direction, σ_k and σ_ε are the turbulent Prandtl numbers for k and ε. μ is the laminar viscosity, μ_t represents the turbulence viscosity, G_k represents the generation of turbulent kinetic energy due to the mean velocity gradients. Adjustable constants used in the equations are $C_\mu = 0.09,\ C_{1\varepsilon} = 1.44,\ C_{2\varepsilon} = 1.92,\ \sigma_k = 1.0,\ \sigma_\varepsilon = 1.3$.

The standard wall functions were used for near the wall treatment (Bacharoudis et al., 2008). The main idea in this study was to optimize the pump parameters; therefore water was used as a working fluid instead of two phase flow. The impeller zone is taken as a rotating zone, which incorporates the pump impeller, with rotational speeds 900 and 1000 rpm. The other zones are stationary. No-slip boundary conditions have been imposed over the impeller blades and the walls (Jafarzadeh et al., 2011). The velocity inlet and pressure outlet boundary conditions were utilized at the inlet and outlet, respectively.

The turbulence intensity and the hydraulic diameter involved parameters are estimated with values of 5% and D, respectively. The numerical algorithm is utilized SIMPLE, (Tekkalmaz, 2015), in which the pressure parameter is discretized using the second-order upwind scheme (Kyparissis et al., 2009; Engin, 2006). The second order upwind scheme is used for spatial discretization. A second order discretization, which presents higher-order accuracy especially for complex flows involving seperation, was used for momentum, turbulent kinetic energy, turbulent dissipation rate (Özmen and Baydar, 2013).

The Calculation of The Pump Performance Curves

After numerical simulations, the characteristic curves of the studied pumps could be calculated with following equations:

Angular velocity : $\omega = \frac{2\pi n}{60}$ (rad/s) (7)

Shaft Power : $P_{sh} = T\times\omega$ (Watt) (8)

Head : $H = \frac{\Delta p}{\rho g}$ (m) (9)

Efficiency : $\eta = \frac{\Delta P\times Q}{P_{sh}\times 3600}$ (10)

The relative error : $_t = \left|\frac{\text{absolute error}}{\text{actual value}}\right| \times 100$ (11)

where n is the number of revolutions per minute (rpm), T is the torque , Δp is the total pressure difference, Q is the flow rate (m^3/h), ρ is the density and g is the acceleration of gravity (Cengel and Cimbala, 2006).

RESULTS AND DISCUSSIONS

The centrifugal slurry pump was operated at two rotational speeds 900 rpm and 1000 rpm in the computations for experimental and parametric study, respectively. The performance curves of the slurry pump while handling clear water is plotted via head-flow rate (H-Q), shaft power-flow rate (P_{shaft}-Q) and efficiency-flow rate (η-Q) curves at several different flow rates. Moreover the flow field inside the pump is visualized with the instantaneous streamlines, velocity vectors and pressure contours. The observation of the flow field gives significant information and hints to the researchers during the design stage.

In this part, the velocity streamlines and the pressure contours through the pumps are presented at the

nominal flow rates in which the hydraulic efficiency of the slurry pump achieves its maximum value, about 125 m^3/h. In fact the nominal flow rates of each impeller are different, but 125 m^3/h was chosen for reference.

Experimental Work

A test rig was established using pump manufacture facilities to test the products. Due to the different sizes of pumps, the experimental test rig established taking into consideration three test units shown in Fig.5. The centrifugal slurry pump with the original impeller was tested with the middle section of the test unit. A water accumulator tank, which was mounted up was used to remove the air flow additionally unsure continuity for obtaining more accurate results within the system. In order to test the original impeller, the test rig was equipped with some devices. There were two pressure transducers to measure the suction and discharge pressures shown in the Fig.5. The flow rate was measured using an electromagnetic flow meter on the water tank. Two shut-off valves were fitted on each test unit. Electrical signals corresponding to the measurement of pressure, flow rate, torque were read by data acquisition/control unit.

At the beginning, the only CAD model of the centrifugal slurry pump was available. For the parametric study, it was decided to create a β_2= 25° impeller with some modification using simple-arc blade design method (SAM) according to the Pfleiderer (1961) blade theory. By the time the performance curves of the original impeller, which experimentally obtained at 900 rpm, were shared towards the end of this study by the company. The analyses of the β_2= 25° impeller had been carried out at 1000 rpm. Moreover a comprehensive CFD analysis of the parametric study was conducted to investigate the effects of blade angle, splitter blade and backward long blades at 1000 rpm.

The head-flow, power-flow and efficiency-flow curves of the original impeller are shown in the Figs.6(a),(b),(c). The best efficient points (BEP) based on the experimental and CFD results were almost 130 m^3/h and 125 m^3/h, respectively. From the head-flow rate curves of two cases, it can be seen that the heads are well correspond to each other between 75-125 m^3/h, however some deviations take place on the other flow

Figure 5.The experimental set-up (left) and the original centrifugal slurry pump(right)

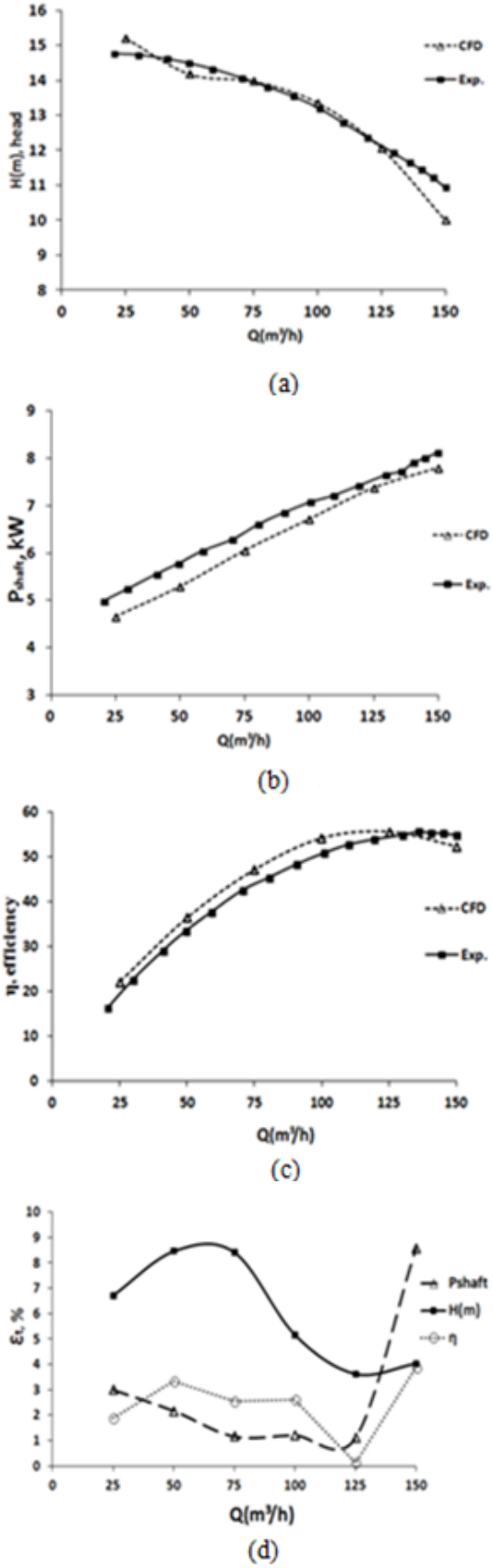

Figure 6. Measured and computed characteristic curves of the original impeller: (a) pump head-flow rate, (b) Pump shaft power-flow rate, (c) pump overall efficiency-flow rate and (d) the relative error at certain flow rates

rates The shaft power values obtained from the experimental study are greater than CFD ones as shown in Fig 6(b). Hence, the efficiency values of the CFD study are greater than the experimental ones as shown in Fig6 (c). The deviation of CFD values based on the experimental data is plotted as relative error-flow rate curves in Fig 6 (d). Although the minimum deviation of the efficiency values takes place at a nominal flow rate, 125m^3/h, the maximum one is taking place at 150 m^3/h.

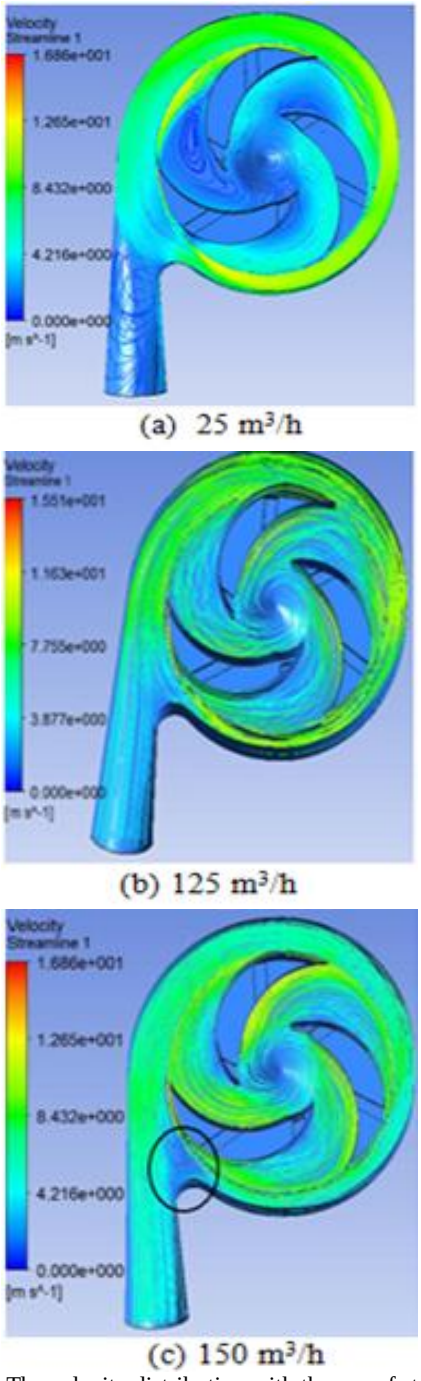

Figure 7. The velocity distribution with the use of streamlines at different flow rates (a),(b) and (c) for the original impeller

The velocity streamlines inside the original impeller for various flow rates is presented as shown in Figs.7(a),(b) and (c). When the pump works at low flow rates, 25 m^3/h, the fluid that comes from inlet part exposes to earlier rotation. Additionally a recirculation zone is established on the pressure side of the leading edge as well as in the volute outlet as shown in Fig.7(a). This situation results in hydraulic energy loss. On the other hand, the flow pattern of the pump is more uniform and steady for 125 and 150 m^3/h. From the velocity streamline, the velocity decreases from the impeller trailing edge to volute exit at each flow rate.

Effects of Blade Outlet Angle on Flow Field at 1000 Rpm

The angle of outlet β_2 can theoretically be selected freely within a wide range; however, in centrifugal pump only backwards curved blades with angles of outlet $\beta_2 = 40° - 20°$ are preferred Benra (2015). In this part the performance of three impellers with different angles of outlet β_2 $(20°, 25°, \text{and } 40°)$ investigated. The velocity streamlines formed throughout the pump for these impellers are presented in Fig.8. It is known that the mechanical energy obtaining from the pump impeller is converted to the pressure energy at the exit of the volute. Therefore,the highest velocity observed at the exit of the trailing edge is decreased towards the exit of the volute as shown in Fig. 8 (a),(b) and (c).

From the flow patterns, it can be deduced that when outlet blade angle increases from $\beta_2 = 20°$ to $\beta_2 = 40°$ the flow is disturbed both at the suction side and at the pressure side of the blades therefore the flow separation occurs on both sides of the blades. This situation is thought to occur because of the blade tip design and the inadequate blade curvature for $\beta_2 = 40°$ impeller as shown in Fig.8 (c). From the Figs.8 (a),(b) and (c), the flow recirculation does not take place obviously almost inside the impellers and volutes. This situation is estimated to result from on design conditions.

The variances of the performance curves versus the flow rate for numerically studied impellers at design and off design conditions are shown in Figs.9(a),(b) and (c). It is obviously seen from Fig.9(a) that the head of the pump decreases with the increment of flow rate as expected. Additionally the decrease of the head depends significantly on the β_2. From the Fig. 9 (a), the head pressure decreases with an increment of angle β_2 up to bep, however, after the bep, the situation almost reverses. The head of $\beta_2 = 20°$ impeller drops off dramatically on the other hand the heads of the $\beta_2 = 25°$ and $\beta_2 = 40°$ impellers decrease gradually.

As for the shaft power-flow rate in Fig.9(b), the $\beta_2 = 40°$ impeller operates with more shaft power than others. Though the shaft power of the $\beta_2 = 25°$ impeller is less than one of $\beta_2 = 20°$ impeller about nominal flow rate, (125 m^3/h), the situation reverses at high flow

rates because of the high frictions between fluid and curvature blade surfaces. This situation also negatively affects the efficiency of the pump at high flow rates.

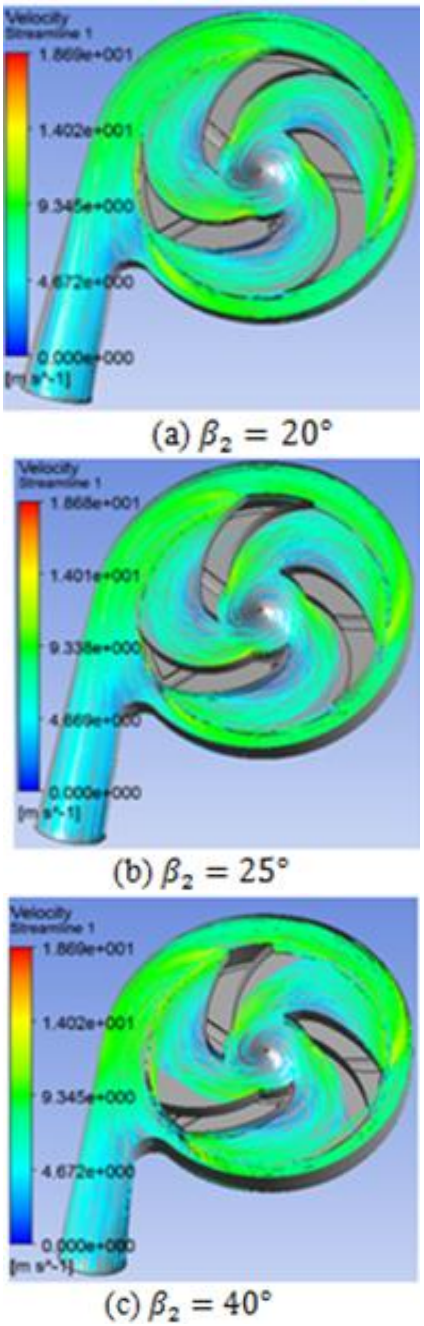

Figure 8. The velocity streamlines of the centrifugal slurry pumps for three outlet blade angles at nominal flow rates (125m^3/h)

The efficiency-flow rates curves are depicted in Fig.9(c). From the curves, the efficiency of the $\beta_2 = 20°$ impeller is better than $\beta_2 = 25°$ and $\beta_2 = 40°$ impellers until the nominal flow rates (125 m^3/h). Because it is shown from the Fig.9(a) and (b) that the head of $\beta_2 = 20°$ impeller is maximum additionally the shaft power of this impeller is minimum up to bep. However, after this point (bep), the efficiency of the $\beta_2 = 20°$ impeller declines sharpen than the others ($\beta_2 = 25°$ and $\beta_2 = 40°$) and it is the most inefficient at high flow rates (175 m^3/h-200 m^3/h). It is seen from the Fig.9 (c) that with the change of β_2, the location of the bep point of the impeller also changes. The bep point of impeller moves the right with the increase of β_2 angle. At the three nominal flow rates (125 m^3/h, 140 m^3/h and 150 m^3/h), the value of the hydraulic efficiencies of $\beta_2 = 20°$,$\beta_2 = 25°$ and $\beta_2 = 40°$ impellers are 65.8%, 64.6% and 59.5%, respectively. The $\beta_2 = 40°$ impeller is not almost demonstrating a good performance neither at low flow rates nor at high flow rates compared to the $\beta_2 = 20°$ and $\beta_2 = 25°$ impellers.

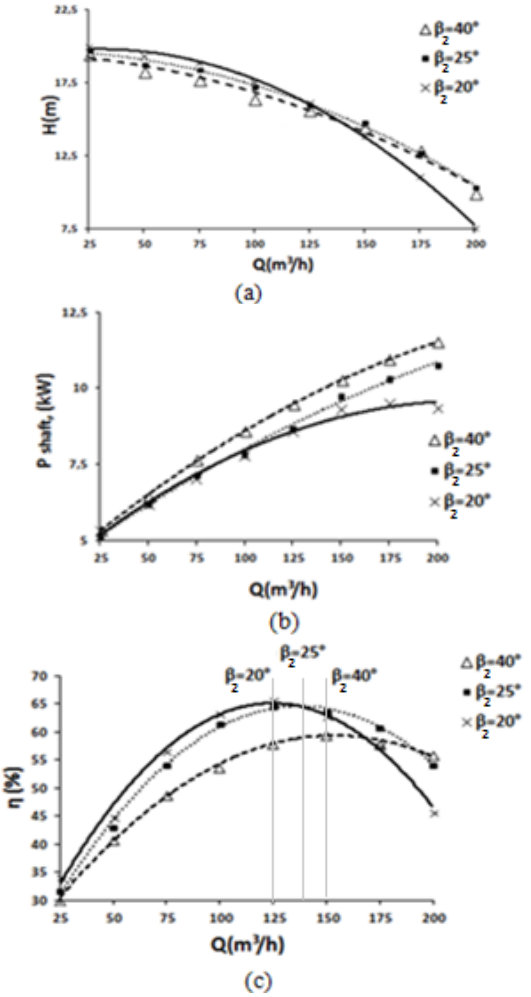

Figure 9. Performance curves of centrifugal slurry pump for $\beta_2 = 20°, \beta_2 = 25°$ *and* $\beta_2 = 40°$ impellers

Effects of Splitter Blades by $1/2$ and $1/1$ Blade Height on Flow Patterns at 1000 Rpm

Figs.10 shows the velocity vectors in the SP1 and SP2 impellers at three plane sections 5 mm, 10 mm and 15,5 mm, respectively. It is clearly seen that the tip leakage flow is occurring because of the tip clearance of the splitter blades of SP1 as shown in Figs.10(c). This situation likely gives rise to total pressure decrease because of the friction losses between the fluid and splitter blades (Engin, 2006). On the other hand, when

the SP2 impeller is employed, the tip leakage is annihilated by the shroud.

The performance curves of the centrifugal slurry pump for β_2= 25°, SP1 and SP2 impellers are shown in Figs.11(a), (b) and (c), where the effects of splitter blades are clearly observed. The addition of splitters has a positive effect on the pump head as shown in Fig. 11(a). Because adding splitters increases the impeller slip factor which helps conduction of the flow Kergourlay et al. (2007). On the other hand, the addition of splitters increases the shaft power as shown in Fig. 11(b). Additionally the height of the splitter also affects the head and shaft power.

In spite of increasing the head of the pumps, more shaft powers are required for SP1 and SP2 impellers in comparison to the β_2= 25° impeller. Therefore SP1 and SP2 have not remarkable effects on the hydraulic efficiency compared to the β_2= 25° impeller till to nominal flow rate (125m^3/h), but the situation changes at high flow rates. From the results, the addition of splitter blades by 15mm blade height increases the head of the β_2= 25° impeller by 5.5%, and the hydraulic efficiency by 1%. On the other hand SP2 impeller increases the head of the β_2= 25° impeller by 13%, but decreases the hydraulic efficiency by 1% in the nominal flow rate (125m^3/h). However the SP2 impeller increases the head and hydraulic efficiency of the β_2= 25° impeller by 17% and 4%, respectively at the 175 m^3/h.

Effects of Backward Long Blades and New Tongue Region on Flow Patterns at 1000 Rpm

During the analysis of the original and β_2= 25° impellers, it is observed that the leading edge and the curvature of the blades are not well corresponding to the fluid flow field resulted from the three critical points presented as a, b and c in Fig.12(a). The flow pattern near points b and c is thought to be disrupted, resulting from the leading edge and insufficient blade curvature.

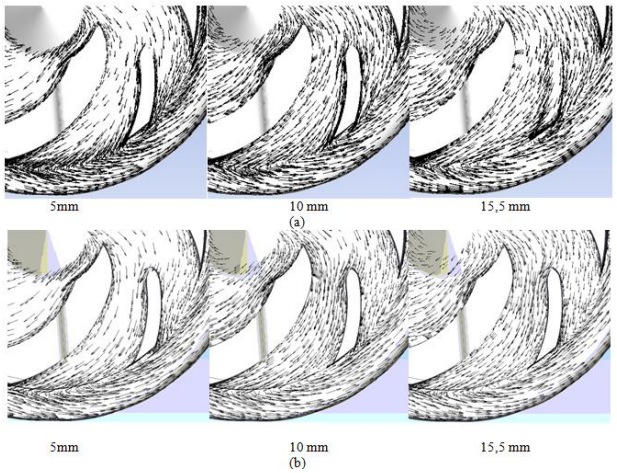

Figure 10. Velocity vectors for SP1 (a) and SP2 (b) impellers at z=5mm, 10 mm and 15,5 mm planes

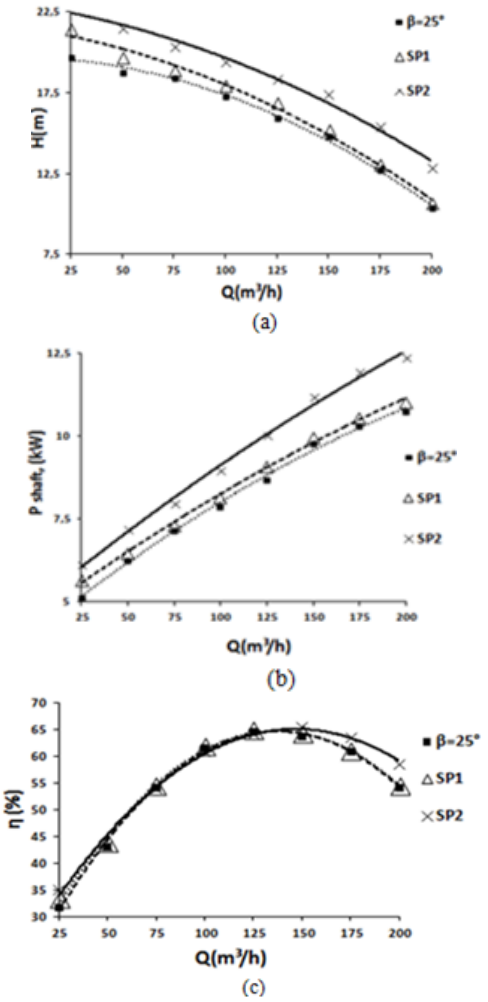

Figure 11. Performance curves of the centrifugal slurry pumps for $\beta_2 = 25°$, SP1, and SP2 impellers

Therefore, it was required to design a new blade configuration. After the modification of the β_2= 25° impeller, the name of the impeller is changed as backward long blades (BLB) impeller as shown in Fig.12(b). With the use of BLB impeller, it is noticed that the flow pattern inside the pump becomes more steady compared to the β_2= 25° impeller. The flow distortion is considerably eliminated not only about the leading edge, but also in the flow passage. Consequently, the flow pattern in the BLB impeller is getting better by the new blade profile.

The volute tongue region, which demonstrates a recirculation of the fluid particles at the gap between the volute tongue and the impeller circumference Kergourlay (2007), has a significant impact on the pump performance. The designing of tongue region of the centrifugal slurry pump generally depends on the slurry mixture and physical properties of solids like their specific gravity (S), shape, particle size (d_{wn}, d_{50}) and size distribution of particles. It needs to a special attention to designing. In this study, in order to reduce hydraulic energy loss due to the recirculation, the tongue radius is reduced as shown in Fig.13. To evaluate the performance of BLB impeller and new volute, the performance curves of pumps are compared

in Fig.14. Fig.14(a) shows that the head of the pump is increased by the BLB impeller up to the nominal flow rate (125m^3/h), but after this flow rate the situaion reverses. The head of the pump does not change with the configured tongue region. On the other hand the required shaft power for BLB impeller is less than the β_2= 25° impeller almost at entire range of flow rate. The required shaft power is minimized when a new tongue region is used in additional to the BLB impeller (BLB+NV) as shown in Fig.14(b). The modification of the volute tongue radius and tongue leading edge do not affect the head as much as the efficiency as shown in Fig.14(a) and (c).

At the nominal flow rate (125 m^3/h), the head and hydraulic efficiency of the β_2= 25° impeller increased by BLB impeller by 2.3% and 5.8%, respectively. In additional to utilize the BLB impeller, with the use of modified volute the head and hydraulic efficiency of the pump (β_2= 25° impeller) increases by 2% and 9% respectively.

In additional to velocity streamlines, the instantaneous static pressure variations within the pump and impellers are presented in Fig.15 for all impellers except for original impeller which is presented above.

From the pressure contours, although pressure distributions from the inlet areas to volute outlet areas of the pumps are almost the same, they are not the same for the impellers because of the blade configurations and splitter blades. It is seen from the head-flow rate curves presented above that the maximum pressure consists with the use of SP2 impeller. Therefore, the legend demonstrated in the Fig.15 belongs to the SP2 impeller at the nominal flow rate (125m^3/h). The static pressure is gradually increased from impeller eye to impeller outer diameter for each pump shown in Fig. 15. Moreover, it can be seen that the low pressure is prevailed at impeller eye and at the suction side of the blades. On the other hand, the high static pressure occurs at the volute exit and the pressure side of the blades. Although the splitter blades increase the friction losses and the required extra shaft power result from energy loss mentioned previously, they contribute the total pressure increases inside the pump since the splitter blade acts as almost blades (Madhwesh et al., 2011; Kergourlay et al., 2007).

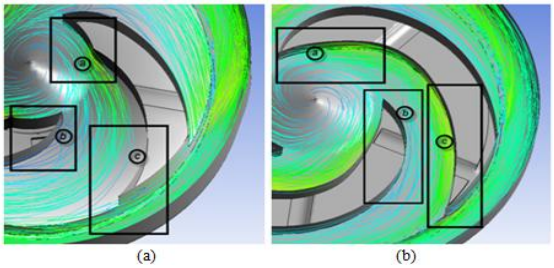

Figure 12. The velocity streamlines distribution for β_2= 25° (a) and BLB impellers (b)

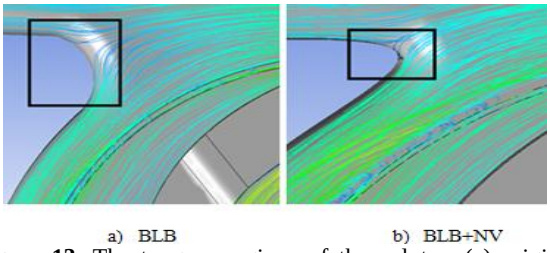

Figure 13. The tongues regions of the valutes: (a) original tongue region (b) re-designed one for the BLB impellers

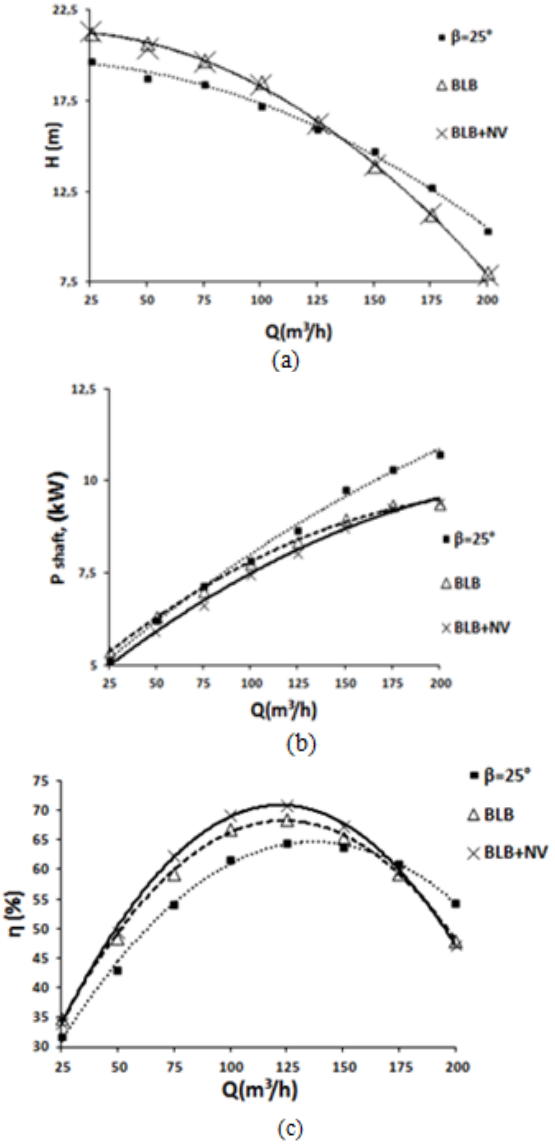

Figure 14. Performance curves of the centrifugal slurry pumps for β_2= 25° and BLB impellers, and backward long blades with new volute (BLB+NV)

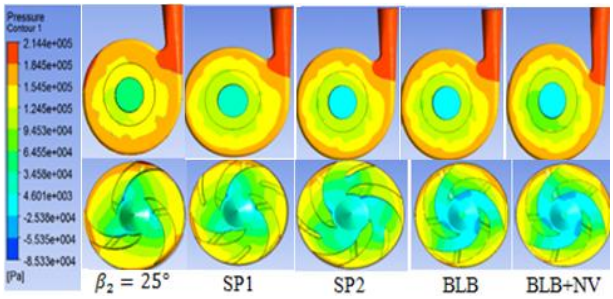

Figure 15. The instantaneous static pressure contours for pumps and impellers

A CASE STUDY: THE PERFORMANCE CURVES OF CENTRIFUGAL SLURRY PUMP WHILE HANDLING SLURRIES

Generally, the selection of the pump based on the pump performance curves obtained with clear water only. However, the performance curves of a centrifugal slurry pump differ from its clear water when solids are included and the flow becomes two phases. To predict the performance of a centrifugal slurry pump while handling settling slurries, some correlations were recommended by researchers (Engin, 2001; Vocadlo et al., 1974; Cave, 1976; Burgess and Reizes, 1976; Sellgren, Gahlot et al., 1992). With the use of these correlations when pumping slurries, it is a way to predict the performance curves of the slurry pump with the use of reduction factors (K_H, K_η), which are mainly function of weighted or volumetric concentration of solids (C_w, C_v) in mixture, physical properties of solids like their specific gravity (S), shape, particle size (d_{wn}, d_{50}) and size distribution of particles. The head and the efficiency reduction factors can be defined by the following expressions (Kazim et al., 1997; Engin, 2001).

$$K_H = 1 - H_r = 1 - \frac{H_S}{H_W} = f\ \ C_w, S, \frac{d_{wn}}{D} \quad (12)$$

$$K_\eta = 1 - \eta_r = 1 - \frac{\eta_S}{\eta_W} = f\ \ C_w, S, \frac{d_{wn}}{D} \quad (13)$$

Where subscripts s and w represents the slurry and water, respectively. The efficiency ratio (η_r) of a slurry pump has been reported by some earlier investigators (Kazim et al., 1997) to be nearly equal to the corresponding head ratio (H_r). Because of that the correlations given in the literature only predict H_r or K_H to obtain pump performance characteristics in slurry services (Kazim et al., 1997). Some recommended correlations to predict the performance reduction factors are given by

Cave : (14)

$$K_H = 0.0385(S-1)\frac{(5+4)}{5} C_w \ln \frac{d_{50}}{22.7}$$

Kazim et al. : $K_H = 0.13 C_w \sqrt{S-1} \ln \frac{d_{wn}}{20}$ (15)

Engin and Gur: $K_H = 0.11 C_w (S-1)^{0.64} \ln \frac{d_{wn}}{22.7}$ (16)

In additional to evaluating the performance characteristics of the centrifugal slurry pump (β_2= 25° impeller) as clear water is working fluid, the performance curves of the slurry pump is calculated while handling slurries including sand D, sand E and mild steel based on the correlation of Kazim et al. (1997) as shown in Fig.16 and Fig.17. The specific features of these solids are presented in Table 3.

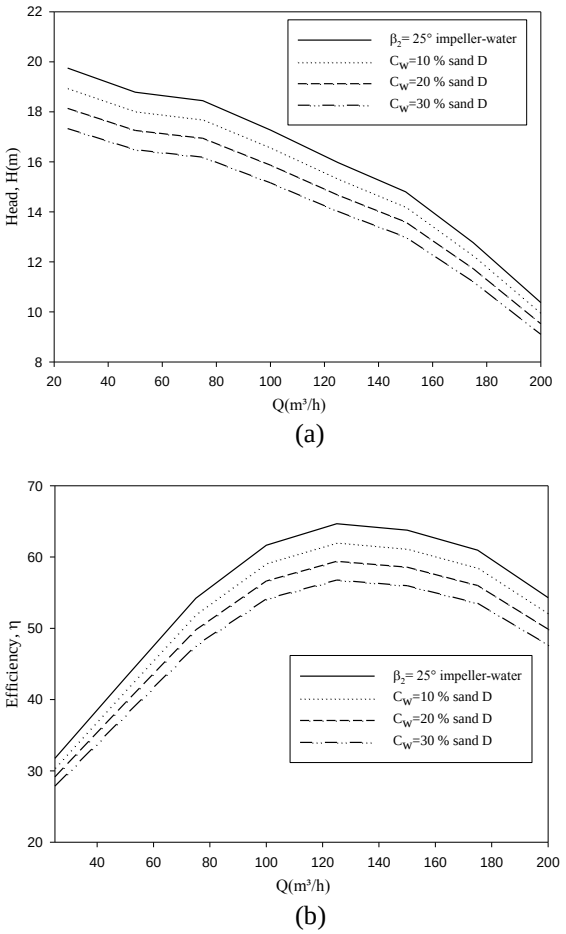

Figure 16. The head-flow rate and the efficiency-flow rate curves of the slurry pump (β_2= 25° impeller) at different concentrations of Sand-D

The performance curves of the β_2= 25° impeller while handling clear water and different slurry concentrations of sand D (10%, %20, %30) are presented in Fig.16. From the curves it is seen that the maximum head and efficiency of the slurry pump is obtained with the clear water. On the other hand, the head and efficiency of the slurry pump decrease with the addition of sand D. Moreover with the increase in solid concentration causes further decreases in the performance of the slurry pump.

It can be seen in the Fig.17 that the addition of the each solid materials (sand D, sand E and mild steel) to the water causes to decrease the pump head and efficiency of the pump as compared to clear water. The decrease in the head and efficiecny of the pumps are different from each other due to distinct specific gravities and particle sizes. The head and the efficiency of the pump decrease while the particle size increased from 230 μm (sand D) to 328 μm (sand E). Additionally the increment in specific gravity from 2.65 (sand D, sand E) to the 6.24 (mild steel) causes to decrease of the slurry pump performance.

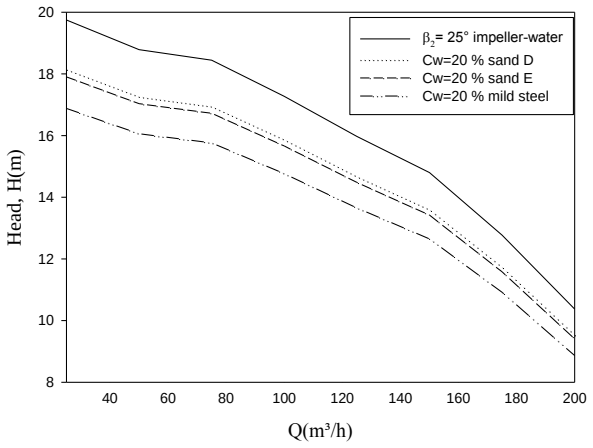

(a)

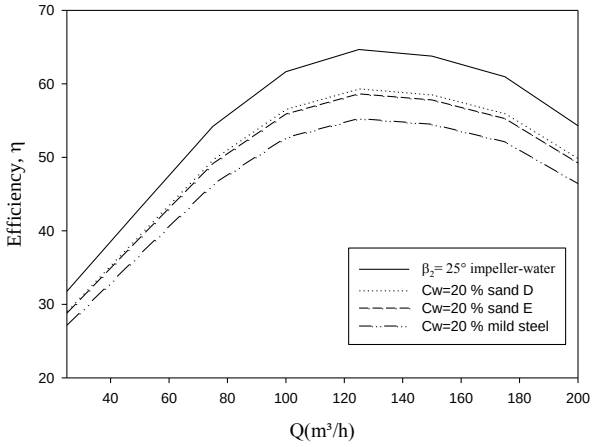

(b)

Figure 17: The head-flow rate and the efficiency-flow rate curves of the slurry pump (β_2= 25°) at 20% concentration of three solid materials

Table 3: Solid materials and characteristics (Kazim et al. 1997)

Solid materials	S	d_{wn} (μm)	c_w (%)
Sand D	2.65	230	10-30
Sand E	2.65	328	20
Mild Steel	6.24	230	20

In the light of the above information the performance characteristics of slurry pump on the working condition while handling clear water and three solid materials slurries with various physical properties are compared in the table 4.

Table 4: Performance characteristics of centrifugal slurry pump (β_2= 25°) while handling water or slurries.

Materials	C_w (%)	S	d_w (μm)	Efficiency (%)	Head (m)	Reduction (%)
Water	-	-	-	64.676	15.971	-
Sand-D	20	2.65	230	59.400	14.668	8.158
Sand-E	20	2.65	328	58.634	14.479	9.341
Mild steel	20	6.24	230	55.274	13.649	14.538

From the table 4, it can be seen that the performance of slurry pump while handling clear water is maximum then it becomes to decrease with the addition of solid particles at low or high concentrations. It is deduced that not only the concentration but also the particle size and specific gravity of the slurries have a strong impact on the performance characteristics of the slurry pump.

CONCLUSION

This study investigates the performance characteristics of an original centrifugal slurry pump experimentally and numerically. Then an extensive numerical investigation to optimize the hydraulic efficiency of the centrifugal slurry pump impeller has been carried out considering the outlet blade angle(β_2), the splitter blades and the modified blades (backward long blades). The numerical solutions of the discredited three-dimensional, incompressible Navier-Stokes equations over a structurel grid is accomplished with ANSYS-Fluent. After the computations, the flow pattern through the pumps is visualized with the streamlines and instantaneous pressure contours. Additionally, the characteristic performance curves of each impeller is compared and discussed.

The effect of the outlet blade angle (β_2) on the performance of the impeller varies from low flow rates to high flow rates. Until the high flow rate (160 m^3/h), the decrease in outlet blade angle, from 40° to 20°, increases the head and the hydraulic efficiency, however, it becomes worse after the this point. At nominal flow rate (125 m^3/h), a 20° decrease in the parametric impeller, from 40° to 20°, causes a 10.6% increase of the hydraulic efficiency. Thus, it seems that the selection of the β_2 angle is crucial for the impeller performance.

This study shows that the blade height of the adding splitters is one of another important parameter affect on the centrigufal slurry pump charactertics. The adding splitters (15mm or 30 mm) increase the pump head and shaft power at any flow rates. Although adding splitters by 15 mm blade height has not a remarkable effect on the pump performance characteristics, the adding splitters by 30 mm blade height increase the head and the shaft power remarkably for the whole range of flow rate. On the other hand, adding splitters on the β_2= 25° impeller by 30 mm blade height increases the hydraulic efficiency remarkably only at high flow rates (150 m^3/h-200 m^3/h).

One of the most important result of this study is modifying the leading edge of the blades which probable causes the flow disruption. With the modify of leading edge and curvature of the blade, the hydraulic efficiency of β_2= 25° impeller has been increased about 6% (BLB impeller).

Apart from impeller, the volute of the pump is another important part which directly affects the pump performance. It is found that with the use of BLB

impeller, if the tongue region of the volute is redesign to prevent the flow directed into the impeller, the hydraulic efficiency of the pump which utilizes the β_2= 25° impeller, can be increased totally about 9% at the nominal flow rate (125m^3/h).

The performance characteristics of slurry pump while handling clear water is the maximum then it becomes to decrease with the increment in the concentrations of solid materials. Not only the concentration but also the particle size and specific gravity of the slurries have a strong impact on the performance characteristics of the slurry pump.

Finally, in addition to pump performance curves of the slurry pump obtained by clear water, the performance curves prepared in accordance with the type of slurry to be used should be taken into consideration in the selection of the pump.

The authors' future activities will involve a detailed numerical study on blade configuration such as blade height and blade thickness for original impeller. Additionally the performance of the slurry pump will be investigated considering two phase flow.

ACKNOWLEDGEMENTS

The authors are thankful to Scientific and Research Council of Turkey (TUBITAK-TEYDEP-3110368) and Company of Tufekcioglu Kaucuk Ltd for their supports on this research.

REFERENCES

Bacharoudis E. C., Filios A. E., Mentzos M. D. and Margaris D. P., 2008, Parametric Study Of A Centrifugal Pump Impeller By Varying The Outlet Blade Angle, *The Open Mechanical Engineering Journal*, 2, 75-83.

Cui B., Zhu Z., Zhang J. and Chen Y., 2006, The flow simulation and experimental study of low-Specific-speed high-speed complex centrifugal impellers, *Chinese journal Chemical Engineering*, 14, 435-441.

Benra F. K., 2015, *Practical Course Turbomachinery, Measurement Of The Characteristics Of A Centrifugal Pump,* University Duisburg-Essen Faculty of Engineering Sciences Department of Mechanical Engineering, https://www.unidue.de/sm/Downloads/Praktika/Centrifugal_Pump.pdf.

Burgess K. E. and Reizes A., 1976, The Effect Of Sizing, Specific Gravity And Concentration On The Performance Of Centrifugal Pumps, *Proc. Inst. Mech. Eng*, 190, 391-399.

Cader T., Masbernat O. and Roco M. C., 1994, Two-Phase Velocity Distribution And Overall Performance Of A Centrifugal Slurry Pump, *Journal of Fluid Engineering (ASME)*, 116, 316-323.

Cave I., 1976, Effects Of Suspended Solids On The Performance Of Centrifugal Pumps, *Proc. Hydro Transport-4,paper H3, BHRA Fluid Engineering.*

Cengel Y.A. and Cimbala J. M., 2006, *Fluid Mechanics Fundamentals and Applications*, McGraw Hill, New York.

Das L. G., Rawat M. K. and Kuri N., 2011, Flow Analysis of a Centrifugal Slurry Pump While Handling Clean Water at Design and Off-Design Conditions, *The 11 th Asian Int. Conference on Fluid Machinery and The 3rd Fluid Power Technology Exhibition*, IIT Madras, Chennai, India.

Engin T., 2000, *Eperimental Investigation of Centrifugal Pumps When Handling Solid-Liquid Mixtures,* Ph.D. Thesis, Sakarya University, Sakarya, Turkey.

Engin T. and Gur M., 2001, Performance Characteristics Of A Centrifugal Pump Impeller With Running Tip Clearance Pumping Solid-Liquid Mixtures, *Journal of Fluids Engineering*, 123, 532-539.

Engin T., 2006, Study Of Tip Clearance Effects In Centrifugal Fans With Unshrouded Impellers Using Computational Fluid Dynamics, *Proc. IMechE Part A: Journal of Power and Energy*, 220, 599-610.

Fluent Inc., 2005, *Fluent 6.2 User Guide*, 2A.

Gahlot V. K., Seshadri V. and Malhotra R. C., 1992, Effect of Density , Size Distribution, and Concentration of Solids on the Characteristics of Centrifugal Pumps, *ASME J. Fluids Eng,*114, 386-389.

Gandi B. K., Sing S. N. and Seshadri V., 2001, Performance Characteristics of Centrifugal Slurry Pumps, *Journal of Fluids Engineering* 123, 271-280.

Gonzalez J., Fernandez J., Blanco E. and Santolaria C., 2002, Numerical Simulation Of The Dynamic Effects Due to Impeller Volute Interaction In a Centrifugal Pump, *ASME Journal of Fluids Engineering*, 124, 348-355.

Jafarzadeh B., Hajari A., Alishahi M. M. and Akbari M. H., 2011, The Flow Simulations of a Low Specific-Speed High-Speed Centrifugal Pump, *Applied Mathematical Modelling*, 35, 242-249.

Kazim K. A., Maiti B. and Chand P., 1997, A Correlation To Predict The Performance Characteristics of Centrifugal Pumps Handling Slurries, *Journal of Power and Energy-Part A*, 211, 147-157.

Kergourlay G., Younsi M., Bakir F., Rey R., 2007., Influence Of Splitter Blades On The Flow Field Of A Centrifugal Pump: Test-Analysis Comparison, *International Journal of Rotating Machinery*, 2007, doi:10.1155/007/85024.

Kyparissis S. D., Douvi E. C., Panagiotopoulos E. E., Margaris D. P. and Filios A. E., 2009, Cfd Flowfield Analysis And Hydrodynamic Double-Arc Blade Design Effects For Optimum Centrifugal Pump Performance, *International Review of Mechanical Engineering (I.RE.M.E.),* 3, 284-292.

Li W. G., 2011, Inverse Design Of Impeller Blade Of Centrifugal Pump With A Singularity Method, *Jordan Journal of Mechanical and Industrial Engineering* 5, 119-128.

Li W. G., 2012, Effects Of Blade Exit Angle And Liquid Viscosity On Unsteady Flow In Centrifugal Pumps, *Proc. IMechE, Part A: Journal of Power and Energy*, 226, 580-599.

Madhwesh N., Karanth K.V., Sharma N.Y. and Member, IAENG., 2011, Impeller Treatment Of For A Centrifugal Fan Using Splitter Vanes-A Cfd Approach, *Proceeding of the World Congress on Engineering*, 3, London, U.K.

Özmen Y. and Baydar E., 2013, A Numerical Investigation On Confined Impinging Array Of Air Jets, *Isı Bilimi ve Tekniği Dergisi*, 33, 65-74

Pfleiderer C., 1961, *Die Kreiselpumpen Fur Flussigketten Und Gase*, Springer, Verlag, Berlin.

Rababa K. S., 2011, The Effects Of Blades Number And Shape On The Operating Characteristic Of Groundwater Centrifugal Pumps, *European Journal of Scientific Research*, 52, 243-251.

Rajendran S. and Purushothaman K., 2012, Analysis Of A Centrifugal Pump Impeller Using Ansys-CFX, *International Journal of Engineering Research & Technology* (IJERT), 1, 1-6.

Safikhani H., 2011, Khalkhali A. and Farajpoor M., Pareto Based Multi-Objective Optimization Of Centrifugal Pumps Using Cfd, Neural Networks And Genetic Algoritms, *Engineering Applications of Computational Fluid Mechanics*, 5, 37-48.

Sellgren A., 1979, Performance Of Centrifugal Pumps When Pumping Ores And Industrial Minerals, *Proc. Hydro Transport-6, paper G1, BHRA Fluid Engineering*, 291-304.

Sheng Y. S., Yu K. F., Hui F. J. and Ling X., 2012, Numerical Research On Effects Of Splitter Blades To The Influence Of Pump As Turbine, *International Journal of Rotating Machinery, 2012, 1-9.* doi:10.1155/2012/123093.

Baocheng S. and Wei J., 2014, Numerical Simulation of 3D Solid-Liquid Turbulent Flow in a Low Specific Speed Centrifugal Pump: Flow Field Analysis, *Hindawi Publishing Corporation Advances in Mechanical Engineering*, 2014, 1-8.

Singh J. P., Kumar S. and Mohapatra S. K, 2011., Computional Investigation of Slurry Pump Handling Bottom Ash, *International Journal of Fluids Engineering*, 3, 241-249.

Singh R. R. and Nataraj M., 2012, Parametric Study And Optimization Of Centrifugal Pump Impeller By Varying The Design Parameter Using Computational Fluid Dynamics: Part I, *Journal of Mechanical and Production Engineering (JMPE)*, 2, 87-97.

Sun J. and Tsukamoto H., 2001, Off-design Performance Predictions For Diffuser Pumps, *Journal of Power and Energy Proceedings of I. Mech. E, Part A*; 215, 191-201.

Tekkalmaz, M., 2015, Numerical Analysis of Combined Natural Convection and Radiation In A Square Enclosure Partially Heated Vertical Wall, *Isı Bilimi ve Tekniği Dergisi,* 35, 99-106.

Tufekcioglu Kaucuk Ltd, 2013.

Versteeg H. K. and Malalasekera W., 1998, *An introduction to computational fluid dynamics*, Longman Group Ltd, England.

Vocadlo J. J., Koo J.K. and Prang A. J., 1974, Performance of Centrifugal Pumps in Slurry Services, *Proc. Hydro Transport-3, Paper J2, BHRA Fluid Engineering.*

Zhou W., Zhao Z., Lee T. S. and Winoto S. H., 2003, Investigation Of Flow Through Centrifugal Pump Impellers Using Computational Fluid Dynamics, *International Journal of Rotating Machinery*, 9, 49-61.

Warman International Ltd., 2000, *Warman Slurry Pumping Handbook*, Australasian Version: Feb.

Mehmet Salih CELLEK is an Research Assistant of Mechanical Engineering at Yildiz Technical University, Turkey. He graduated from University of Sakarya in 2010 with a BSME degree. He received a MSc. degree in 2013 in Mechanical Engineering from Sakarya University. He is currently a Ph.D. student in Heat-Prossess Program in Mechanical Engineering at Yildiz Technical University. His main research areas are turbomachinary, combustion, energy audit and recovery system, heat exchangers, heat transfer and computational fluid dynamics (CFD). He is married and has one child.

Tahsin ENGİN was born in 1968 in Samsun. He received his BSc. degree in Mechanical Engineering from Hacettepe university in 1992 and MSc. degree in Energy branch from Zonguldak Karaelmas (Bülent Ecevit) University and Ph.D. degree also in Energy branch from Sakarya University. He had been worked in Van Cement between 1992-1994 and he had been in Universiy of Nevada/Reno from 2001 to 2003 for his post doctoral research. At the same time he had been worked as a master in the Energy Assesment Center. He have worked in four projects as an administor and in eight project as an investigators. He have received assosiate Professor degree in 2008 then Professor degree in 2013. He have translated two books (Fluid Dynamics/Differantial Equaiton) and these books are awarded by TÜBA for their succesful translation. Tahsin Engin teaches Fluid Mechanics, Differential Equations and Numerical Analysis. He has been working as general menegar in Sakarya Technopolis and manager in ADAPTTO-Tchnology transfer offisce since 2014. Tahsin Engin has more than 80 printed scientific studies and he is married and has 2 children.